This article was downloaded by:
On: *15 January 2011*
Access details: *Access Details: Free Access*
Publisher *Taylor & Francis*
Informa Ltd Registered in England and Wales Registered Number: 1072954 Registered office: Mortimer House, 37-41 Mortimer Street, London W1T 3JH, UK

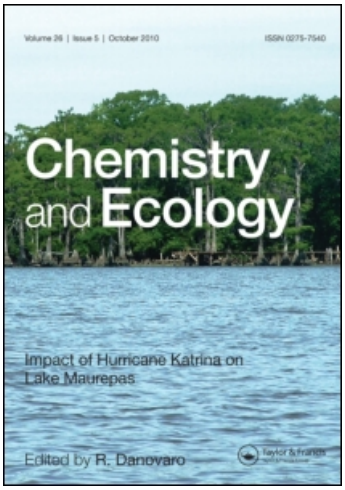


**Chemistry and Ecology**
Publication details, including instructions for authors and subscription information:
http://www.informaworld.com/smpp/title~content=t713455114

# Uptake and desorption of nickel(II) using polymerised tamarind fruit shell with acidic functional groups in aqueous environments

T. S. Anirudhan[a]; P. G. Radhakrishnan[a]
[a] Department of Chemistry, University of Kerala, Kariavattom, Trivandrum, India

Online publication date: 08 April 2010

**To cite this Article** Anirudhan, T. S. and Radhakrishnan, P. G.(2010) 'Uptake and desorption of nickel(II) using polymerised tamarind fruit shell with acidic functional groups in aqueous environments', Chemistry and Ecology, 26: 2, 93 — 109
**To link to this Article: DOI:** 10.1080/02757541003627613
**URL:** http://dx.doi.org/10.1080/02757541003627613

PLEASE SCROLL DOWN FOR ARTICLE

Full terms and conditions of use: http://www.informaworld.com/terms-and-conditions-of-access.pdf

This article may be used for research, teaching and private study purposes. Any substantial or systematic reproduction, re-distribution, re-selling, loan or sub-licensing, systematic supply or distribution in any form to anyone is expressly forbidden.

The publisher does not give any warranty express or implied or make any representation that the contents will be complete or accurate or up to date. The accuracy of any instructions, formulae and drug doses should be independently verified with primary sources. The publisher shall not be liable for any loss, actions, claims, proceedings, demand or costs or damages whatsoever or howsoever caused arising directly or indirectly in connection with or arising out of the use of this material.

*Chemistry and Ecology*
Vol. 26, No. 2, April 2010, 93–109

Taylor & Francis
Taylor & Francis Group

# Uptake and desorption of nickel(II) using polymerised tamarind fruit shell with acidic functional groups in aqueous environments

T.S. Anirudhan* and P.G. Radhakrishnan

*Department of Chemistry, University of Kerala, Kariavattom, Trivandrum 695 581, India*

(*Received 30 April 2009; final version received 12 January 2010*)

Downloaded At: 12:03 15 January 2011

The sorption potential of formaldehyde polymerised tamarind fruit shell (FPTFS) containing acidic functional groups for the treatment of Ni(II) ions from aqueous solutions has been investigated. The adsorbent was characterised by infrared spectroscopy and scanning electron microscopy. Operating parameters affecting Ni(II) adsorption were investigated by the batch technique. Maximum Ni(II) sorption was found to occur at an initial pH of around 6. Kinetic studies showed that the amount adsorbed increased with initial Ni(II) concentration and the equilibrium was established in 180 min. The kinetic data were analysed using the Lagergren pseudo-first-order, Ritchie second-order and modified Ritchie second-order equations, and showed better fit with the modified Ritchie second-order equation. Equilibrium data were analysed by Langmuir, Freundlich, Sips and Toth isotherm models and the Sips model best defined the isotherm. The adsorption of Ni(II) was endothermic in nature ($\Delta H_{ads}$: 45.93 kJ/mol) with an increase in entropy ($\Delta S_{ads}$: 245.67 J/mol/K) and a decrease in Gibbs free energy ($\Delta G_{ads}$: $-28.52$ to $-35.67$ kJ/mol) in the temperature range 30–60 °C. The reduction in adsorption capacity with an increase in ionic strength and isosteric heat of adsorption ($\Delta H_x$: 24.85 kJ/mol) revealed an ion exchange mechanism for Ni(II) adsorption. The adsorption efficiency of FPTFS towards Ni(II) removal from a nickel-plating industry wastewater sample was investigated and quantitative removal of 100 mg/L of Ni(II) in 1 L of industrial wastewater was possible with 6 g of FPTFS. The spent, nickel-laden FPTFS was regenerated by 0.1 M HCl and four adsorption/desorption cycles were performed. The results indicated that FPTFS exhibited considerable potential for application in the removal of Ni(II) ions from aqueous solutions.

**Keywords:** tamarind fruit shell; nickel(II); adsorption kinetics; isotherm; thermodynamics; regeneration

## 1. Introduction

The discharge of toxic heavy metal ions into aquatic environments is nowadays causing serious health hazards to both human beings and animals. The high mobility of these metal ions in water streams and the bioaccumulating nature of these metal ions in animal bodies create a serious impact on aquatic and terrestrial organisms. Nickel is a toxic heavy metal present in industrial wastewaters, and significant amounts of nickel-containing wastewaters are discharged into aquatic streams from Ni-plating plants, silver refineries, nickel battery production plants, mining areas and metal finishing industries [1]. The concentration of nickel ions in industrial wastewaters usually ranges from 3.40 to 900 mg/L [2]. Higher concentrations of nickel cause lung cancer, dizziness,

*Corresponding author. Email: tsani@rediffmail.com

ISSN 0275-7540 print/ISSN 1029-0370 online
© 2010 Taylor & Francis
DOI: 10.1080/02757541003627613
http://www.informaworld.com

cyanosis, nausea and vomiting [3]. Recently, the Environmental Protection Agency has fixed the maximum contamination limit of nickel in potable water as 50 μg/L [4]. Ni concentrations in highly contaminated freshwater may reach as high as several hundred to 1000 μg/L [5]. Hence, there is a great need to treat industrial effluents containing Ni(II) ions before discharging into aquatic streams so as to reduce the Ni(II) ion concentration to below the permissible limits.

Although many established conventional wastewater treatment technologies are available, adsorption is an effective and simple technique for removing metal ions from aqueous solutions. Wastewater treatment using activated carbon or ion exchange resin, although effective, is not economic, and this constraint has caused the search for cost-effective adsorbents for wastewater treatment. Recently, Bailey et al. [6] reviewed the utility of low cost natural materials as sorbents for wastewater treatment. In recent years the use of agricultural by-products for the removal of toxic metals from wastewater has attracted many studies because they are cheap, simple, sludge-free and involve small initial cost. The major component of these agricultural waste by-products includes cellulose, a natural biopolymer having ion exchange properties [7]. Since the adsorption process involves numerous surface interaction mechanisms and diffusion processes, the surface functional groups play a major role in the adsorption process [8]. Chemical conversion of the existing functional groups on the agricultural biomass is generally employed to improve the sorptive potential of many agricultural by-products. Shukla et al. [9] reported the adsorption of Ni(II), Zn(II) and Fe(II) on oxidised coir fibres, and Ali Kara et al. [10] studied the adsorption of Ni(II) ions onto phenolated wood resin. Ewecharoen et al. [11] compared the adsorption of Ni(II) from electroplating rinse waters by coir pith and modified coir pith and showed a high adsorptive capacity for alkali-treated coir pith. Adsorption of Ni(II) using HCl treated oak (*Quercus coccifera*) sawdust was reported by Mehmet Emin Argun et al. [12]. Chitosan modified with Reactive Blue 2 dye was used for the adsorption of Cu(II) and Ni(II) ions [13].

Tamarind (*Tamarindus indica*) is a common tree found in most parts of India. It is basically cultivated for its sour fruit pulp. Tamarind fruit shell (TFS), a byproduct of the tamarind pulp industry, is an underutilised waste material. These waste materials create increasing disposal and potentially severe pollution problems. A large amount of TFS is burnt *in situ*, generating $CO_2$ and other forms of pollution. Any attempt to reutilise the TFS would be worthwhile. In this study, we attempted to develop a TFS-based cation exchanger possessing a $–SO_3H$ functional group for water treatment. The feasibility of the modified TFS for removing Ni(II) ions from water and wastewater was investigated, and operational parameters affecting adsorption process were optimised through a batch process.

Downloaded At: 12:03 15 January 2011

## 2. Materials and methods

### 2.1. *Materials*

TFS collected from a local market was used for the preparation of the adsorbent. The chemicals used throughout the study were of analytical grade. Formaldehyde, 39% (HCHO) and $H_2SO_4$ were procured from E. Merck (India) and $NiCl_2$, $6H_2O$ for preparing the stock solution was obtained from Fluka (Switzerland). Unless otherwise mentioned, all the working solutions were prepared using distilled water. The pH of the working solutions was adjusted using 0.1 N HCl and 0.1 N NaOH solutions.

### 2.2. *Preparation of the adsorbent*

TFS was washed with distilled water to remove the surface impurities and dried at 80 °C. The dried mass was powdered and particles of 80–230 mesh size were collected for chemical treatments.

Two parts of TFS was treated with 20 parts 0.2 N $H_2SO_4$ and five parts 39% HCHO. The reaction mixture was stirred vigorously and heated in a water bath at 60 °C for 6 h. The formaldehyde polymerised TFS containing sulphonic acid group (FPTFS) was washed repeatedly with distilled water to remove unreacted HCHO and $H_2SO_4$, and dried at 60 °C. The dried product was powdered, sieved, and particles of 0.096 mm were used for batch studies.

### 2.3. *Equipment and methods of characterisation*

The FTIR spectra of the TFS and FPTFS were obtained using the pressed disc technique in a Perkin Elmer IR–180 spectrophotometer. The scanning electron micrographs (SEM) for adsorbents were obtained on a Philips XL-3CP scanning microscope at an accelerating voltage of 12 kV. A potentiometric titration method [14] was used to determine the point of zero change ($pH_{pzc}$). The surface area of the adsorbent was determined using a Quantasorb surface area analyser (QS/7). The cation-exchange capacity (CEC) was determined by the column process using 1.0 M $NaNO_3$ as the eluent at a flow rate of 0.5 mL/min [15]. The apparent density of the adsorbents was also determined by specific gravity bottle (10 mL capacity) using nitrobenzene as the displacing liquid. A Systronic microprocessor pH meter (model μ 362; India) was used to measure the pH of the suspension. The total number of acidic groups present in the adsorbents was estimated using a conductometric titration method proposed by James and Parks [16]. A temperature controlled water bath flask shaker (Labline, India) was used for shaking all solutions. The concentration of metal ions in the solution was determined using a GBC Avanta A 5450 (Australia) atomic absorption spectrophotometer (AAS).

Downloaded At: 12:03 15 January 2011

### 2.4. *Adsorption experiments*

Batch adsorption experiments were carried out by shaking 100 mg of FPTFS in 50 mL of Ni(II) solutions with different initial concentrations ranging from 25–600 mg/L in a 100 mL Erlenmeyer flask at 200 rpm in a water bath flask shaker at fixed temperature. The effect of pH on Ni(II) adsorption was studied by varying the initial pH of the solution within the range 2.0–7.0 using 0.1 M NaOH and HCl solutions. After equilibrium, the supernatants were removed by centrifugation and the metal ion concentration was determined using AAS. The optimum lamp current, wavelength and sensitivity of the AAS measurements were 4.0 mA, 232 nm and 0.04 μg/L, respectively. The amount of Ni(II) adsorbed, $q_e$ (mg/g), was calculated using the equation:

$$q_e = (C_o - C_e)\frac{V}{m} \quad (1)$$

where $C_o$ and $C_e$ are the initial and equilibrium Ni(II) concentrations (mg/L), respectively, m is the mass of FPTFS (g) and V is the volume of the solution (L). Kinetic studies were carried out at constant pH, and at room temperature with Ni(II) concentrations ranging from 50–200 mg/L, and at varying temperatures ranging from 30–60 °C using 200 mg/L Ni(II) solution. Samples were withdrawn at different time intervals and the amount of Ni(II) ions in the solution was determined. Isotherm experiments were conducted with 50 mL of different initial concentrations ranging from 50–600 mg/L at 30, 40, 50 and 60 °C.

### 2.5. *Desorption experiments*

To investigate the adsorption mechanism involving Ni(II) removal from aqueous systems using FPTFS and also to make the adsorption process more economic, desorption and regeneration studies were carried out. After adsorption experiments with 25 mg/L Ni(II) using 100 mg of adsorbent in 50 mL aqueous phase, the Ni(II)-laden samples were separated from solutions by

centrifugation and gently washed with distilled water to remove unadsorbed Ni(II) ions. The spent adsorbent was agitated with 50 mL 0.1 M HCl for 3 h. The concentration of desorbed Ni(II) ions in the solution was determined using AAS. The adsorbent thus regenerated was used for further adsorption studies. The adsorption and regeneration cycles were reported four times.

### 2.6. *Nonlinear regression analysis*

The kinetic and isotherm model parameters were evaluated by nonlinear regression using Solver add-in with Microsoft Excel. The model parameters were determined by minimising the distance between the experimental data points and the model predictions. The degrees of fitness of the models with the experimental data were determined using the sum of the squares of errors (SSE), defined as:

$$\mathrm{SSE} = \sum (q_{exp} - q_{cal})^2, \tag{2}$$

and by using the Chi-square test ($\chi^2$), given by:

$$\chi^2 = \sum_{i=1}^{m} \frac{(q_{exp} - q_{cal})^2}{q_{cal}}, \tag{3}$$

where $q_{exp}$ and $q_{cal}$ correspond to the experimental and model data, and m is the number of observations in the experiment. If data from the models are similar to the experimental data, SSE and $\chi^2$ will be a smaller number.

Downloaded At: 12:03 15 January 2011

## 3. Results and discussion

### 3.1. *Adsorbent characterisation*

The functionalisation on TFS was followed through FTIR spectroscopy. The FTIR spectra of TFS and FPTFS are shown in Figure 1. A strong absorption band at 3400 $cm^{-1}$ shows the presence

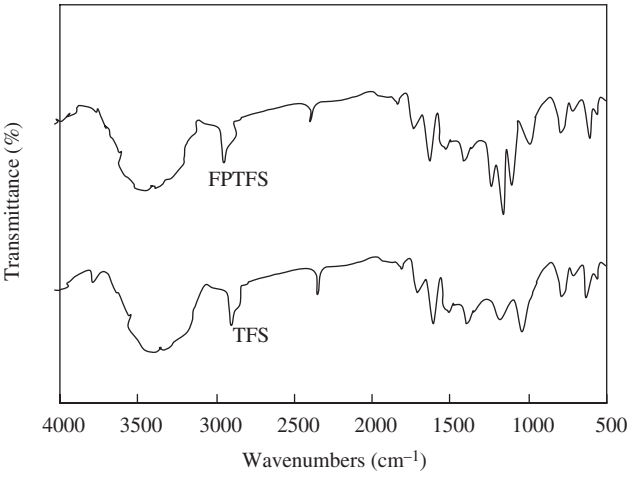


Figure 1. FTIR spectra of TFS and FPTFS.

of hydroxyl groups as part of the cellulose structure and polyphenols originally present in TFS [17]. An absorption band at 2925 $cm^{-1}$ in TFS appeared from the in-phase stretching vibration of $–CH_2$- alkane from cellulose and hemicellulose. A weak absorption band at 1730 $cm^{-1}$ for FPTFS corresponds to the C=O stretching of –COOH group. The characteristic band 1066 $cm^{-1}$ originates from the C–O stretching vibration of –C–OH group. Bands at 677 $cm^{-1}$ for TFS and 673 $cm^{-1}$ for FPTFS arise from $\beta$-glucosidic linkage. The FTIR spectrum of FPTFS shows additional peaks at 1185, 1135 and 605 $cm^{-1}$ showing the presence of $–SO_3H$ group [18]. The absorption band, 1066 $cm^{-1}$ in TFS, shifts to 1033 $cm^{-1}$ in FPTFS due to the reaction of formaldehyde at the cellulosic hydroxyl group.

The surface charge density $\sigma_0$ of TFS and FPTFS was determined by the potentiometric titration method using the equation:

$$\sigma_0 = \frac{F[(C_A - C_B) + (OH^- - H^+)]}{A}, \tag{4}$$

where F is the Faraday constant, and $C_A$ and $C_B$ are the concentrations of acid and base after each addition during titration. $H^+$ and $OH^-$ ions are the equilibrium concentration of $H^+$ and $OH^-$ ions bound to the suspension surface, and A is the surface area of the suspension. The plots of $\sigma_0$ versus pH for TFS and FPTFS are shown in Figure 2. The point of intersection of $\sigma_0$ with the pH curves gives the $pH_{pzc}$ (pH at which surface charge density $\sigma_0$ is zero). The $pH_{pzc}$ of TFS and FPTFS occurred at 7.4 and 5.4 respectively. The decrease in $pH_{pzc}$ after chemical modification indicates that the surface became more negative due to the presence of sulphonate and carboxylate functional groups in FPTFS, and it facilitates the uptake of Ni(II) ions from aqueous solutions through electrostatic interaction.

Downloaded At: 12:03 15 January 2011

The SEM photographs of TFS and FPTFS taken at magnitude 1000× are presented in Figure 3. The FPTFS surface contains numerous scrappy regions which occurred as a result of formaldehyde treatment. These patchy regions were not seen on the surface of TFS. The FPTFS surface was found to have a more dispersed framework with a large number of grooves throughout the surface, which occurred as a result of functionalisation. After formaldehyde treatment, TFS becomes more porous. This porous appearance probably occurs due to the reduction in certain amorphous/crystalline phases originally associated with the TFS.

The surface areas obtained for TFS and FPTFS using $N_2$ sorption were found to be 13.3 and 25.7 $m^2/g$, respectively. The increase in surface area of FPTFS is attributed to the reduction in

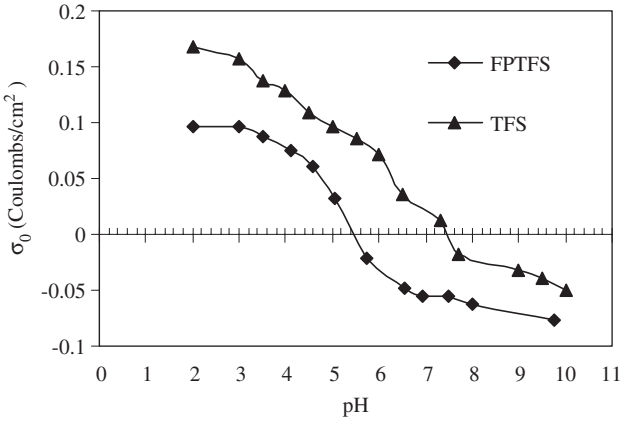


Figure 2. Surface charge density as a function of pH in aqueous solution of $NaNO_3$.

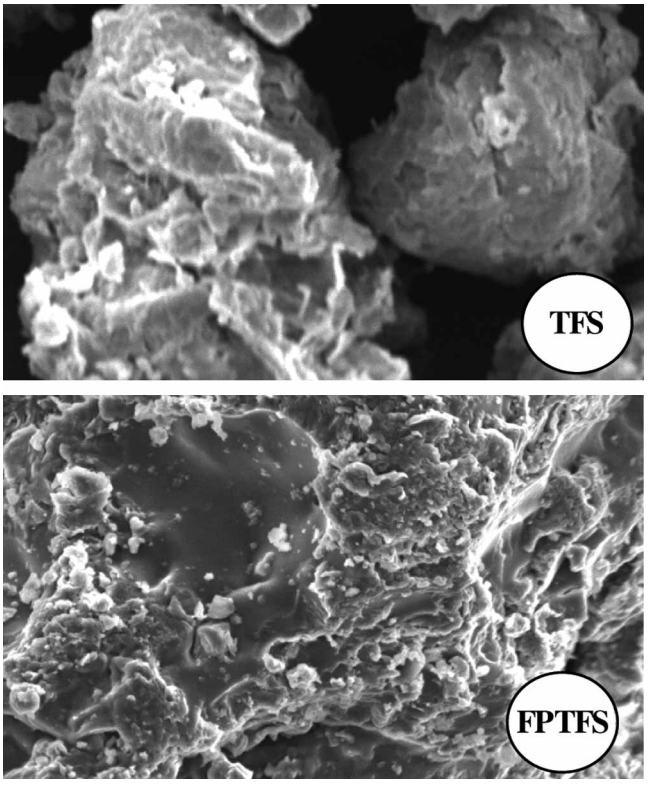


Figure 3. Scanning electron micrographs of TFS and FPTFS.

Downloaded At: 12:03 15 January 2011

crystalline domains, originally present in TFS, on formaldehyde treatment in the presence of 0.2 N $H_2SO_4$. Similar increase in surface area with chemical modification is reported in the literature [19]. The amount of acid groups obtained from conductometric titration was found to be 0.53 and 1.48 meq/g for TFS and FPTFS, respectively. The cation exchange capacities were found to be 0.43 meq/g for TFS and 1.33 meq/g for FPTFS, and this enhancement is consistent with chemical modification, while apparent density was found to be 1.02 and 1.32 g/L for TFS and FPTFS, respectively.

### 3.2. *Effect of surface modification*

The effect of surface modification on Ni(II) adsorption was studied by conducting batch experiments using an initial concentration of 25 mg/L with varying adsorbent doses of TFS and FPTFS. The percentage of adsorption increased with an increase in adsorbent doses, and for the complete removal of Ni(II) ions from aqueous solution, an optimum adsorbent dosage of 3.0 g FPTFS or 4.5 g TFS was required (Figure 4). The increase in removal percentage with doses may be due to the availability of more adsorption sites at high doses. The results clearly show that FPTFS is 1.5 times more effective than TFS for Ni(II) removal from aqueous solutions. The high percentage removal obtained for FPTFS may be due to the stability provided by formaldehyde polymerisation and also due to the introduction of a $–SO_3H$ group on the FPTFS surface through chemical treatment. The values of $pH_{pzc}$ of TFS and FPTFS were found to be 7.4 and 5.4 respectively. The low $pH_{pzc}$ of FPTFS indicates that the FPTFS surface became more negative due to chemical treatment and this increases the extent of Ni(II) adsorption onto FPTFS.

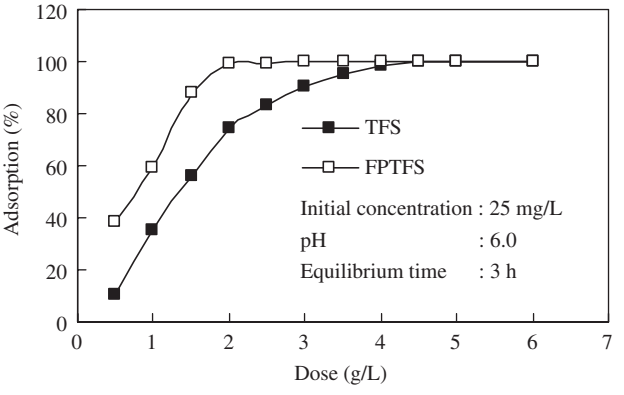


Figure 4. Effect of adsorbent dose on the removal of Ni(II) from aqueous solution by TFS and FPTFS.

### 3.3. *Effect of pH on Ni(II) removal*

Downloaded At: 12:03 15 January 2011

The pH value of the solution plays an important role in the adsorption of metal ions from aqueous solutions. The pH dependence of equilibrium adsorption data of Ni(II) ions in solution is shown in Figure 5, which shows that the amount adsorbed increased with increase in pH and maximum sorption was obtained at pH 6. This trend was attributed to the solution pH influencing both the active sites of FPTFS and the Ni(II) chemistry in water. With increasing pH values, the carboxyl and sulphonic acid groups, would be exposed producing negative charges on FPTFS surface causing enhanced metal sorption [20]. For an initial concentration of 25 and 50 mg/L, the amount adsorbed was found to be 12.39 mg/g (99.1%) and 23.33 mg/g (93.1%), respectively, at pH 6. Lower sorption capacities at lower pH values can be attributed to the competitive sorption of $H_3O^+$ ions and $Ni^{2+}$ ions for the same adsorption sites. With the increase in pH, the competing effect of $H_3O^+$ ions decreases, and hence the cationic Ni(II) ions can bind to the adsorption sites. Ni(II) adsorption is more significant above pH 4. In the pH range 2–7, the major components in the solution are $Ni^{2+}$ species and the hydrolysed forms of $NiOH^+$ and $Ni(OH)_2$ species. The $pH_{pzc}$ of FPTFS occurred at pH 5.4, which indicates that below pH 5.4, the FPTFS surface is positively charged and the main species in the solution, such as $Ni^{2+}$ and $NiOH^+$ ions, get adsorbed on FPTFS through the ion exchange process. A substantial decrease in the experimental pH occurs during adsorption and this may be due to the release of $H^+$ ions from the peripheral –COOH and

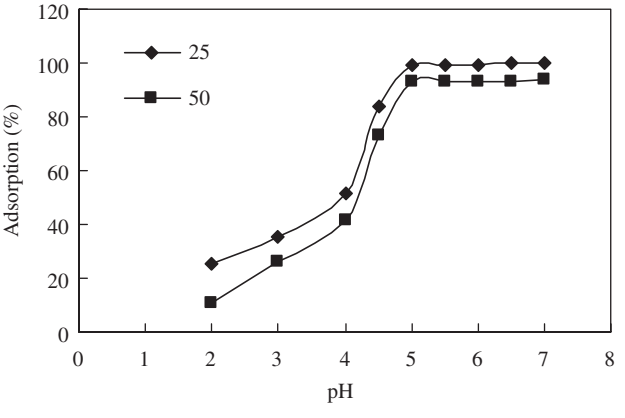


Figure 5. Effect of pH on the adsorption of Ni(II) onto FPTFS.

$-SO_3H$ groups present in FPTFS. The removal of Ni(II) below pH 5.4 may be represented as:

$$2H - FPTFS + Ni^{2+} \rightarrow (FPTFS)_2Ni + 2H^+, \quad (5)$$

$$H - FPTFS + Ni(OH)^+ \rightarrow FPTFS - Ni(OH)^+ + H^+. \quad (6)$$

At pH $>$ 5.4, the FPTFS surface becomes negatively charged and the metal species in the solution exist as $NiOH^+$ ions. Under such conditions, a favourable electrostatic attraction between FPTFS and $NiOH^+$ ions is responsible for metal uptake. Similar adsorption mechanisms for metal removal from aqueous solutions have been reported in the literature [21].

### 3.4. *Effect of initial concentration and contact time*

Figure 6 shows the effect of contact time on the removal of Ni(II) ions from aqueous solutions in the concentration range 50–200 mg/L at pH 6 and 30 °C. For the different initial Ni(II) concentrations (50–200 mg/L), almost 80–85% of the overall adsorption occurred during the 60 min contact time, and subsequently the amount adsorbed slowly increased with time and equilibrium was established at 180 min. The equilibrium time was independent of initial concentration and, for further batch studies, the contact time was fixed as 3 h. The nature of the adsorbent and its compactness also affected the equilibrium time for Ni(II) adsorption. The initial high sorption rate within 60 min may partly be due to the presence of various functional groups on FPTFS, and Ni(II) ions having easy access towards these active sites. For initial concentrations of 50, 100, 150 and 200 mg/L, the equilibrium uptake was found to be 23.26 mg/g (93.1%), 43.28 mg/g (86.6%), 57.82 mg/g (77.1%) and 68.50 mg/g (68.5%), respectively. The results showed that with a rise in initial Ni(II) concentration, equilibrium uptake increased. The enhanced Ni(II) adsorption at higher initial concentration occurs because at higher Ni(II) concentrations, more Ni(II) ions occupy the active sites of FPTFS; further, the presence of a large number of Ni(II) ions in the vicinity of FPTFS surface provides a larger concentration gradient in the liquid film, thus providing a higher driving force for Ni(II) adsorption.

Downloaded At: 12:03 15 January 2011

### 3.5. *Adsorption dynamics*

The kinetic study of metal ion adsorption on solid adsorbents provides valuable information about the adsorption process and its mechanisms. The adsorption data were modelled using the

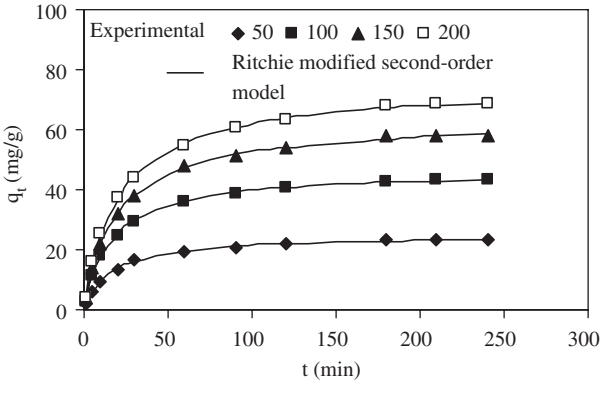


Figure 6. Effect of contact time and initial concentration on the adsorption of Ni(II) onto FPTFS and comparison of the Ritchie modified second-order model with the experimental data.

Pseudo-first-order model [22], the Ritchie second-order model [23] and the Ritchie modified second-order model [24], as shown by the following Equations (7–9):

$$q_t = q_e(1 - e^{-k_1 t}), \tag{7}$$

$$q_t = q_e \left\{1 - \left[\frac{1}{1 + k_2 t}\right]\right\}, \tag{8}$$

$$q_t = q_e \left\{1 - \left[\frac{1}{\beta + k_{2_m} t}\right]\right\}, \tag{9}$$

where $q_e$ and $q_t$ are the amounts of Ni(II) ion adsorbed (mg/g) at equilibrium and time, t, respectively. $k_1$, $k_2$ and $k_{2m}$ are the pseudo-first-order rate constant, the Ritchie second-order rate constant and Ritchie modified second-order rate constant, respectively. $\beta$ is a constant representing the initial particle loading. The kinetic parameters of these models for different initial concentrations were calculated through the nonlinear optimisation method and are given in Table 1. The Ritchie modified second-order model adequately described the kinetics of sorption of Ni(II) for all concentrations with lower SSE and $\chi^2$ values. The applicability of the Ritchie modified second-order model implies that one Ni(II) ion was adsorbed onto two surface sites of FPTFS; this adsorption process could be represented as in Scheme 1.

Earlier studies have successfully applied the Ritchie modified second-order model to the adsorption of cadmium ions onto bone char [24] and the adsorption of Cd(II) by acid-treated jackfruit peel [25]. A comparison between the experimental and calculated values using a best fit Ritchie modified second-order model is shown in Figure 6. The values of the Ritchie modified second-order rate constant decreased from $6.02 \times 10^{-2}$ to $4.76 \times 10^{-2}$ g/mg/min for an increase in initial concentration from 50 to 200 mg/L. The initial particle loading ($\beta$) and equilibrium sorption capacity ($q_e$) also increased from 1.016–1.041 and 24.67–73.98 mg/g, respectively, as the initial Ni(II) concentration increased from 50–200 mg/L.

Downloaded At: 12:03 15 January 2011

Table 1. Kinetic parameters for the adsorption of Ni(II) onto FPTFS.

| | Concentration (mg/L) | | | |
|---|---|---|---|---|
| | 50 | 100 | 150 | 200 |
| $q_{eexp}$ (mg/g) | 23.26 | 43.28 | 57.82 | 68.50 |
| Pseudo-first-order model | | | | |
| $K_1 \times 10^{-2}$ ($min^{-1}$) | 4.81 | 4.71 | 4.18 | 3.98 |
| $q_e$ (mg/g) | 22.30 | 41.38 | 55.67 | 65.75 |
| SSE | 10.05 | 39.24 | 58.59 | 97.88 |
| $\chi^2$ | 1.29 | 2.47 | 3.52 | 4.23 |
| Ritchie second-order model | | | | |
| $K_2 \times 10^{-2}$ (g/mg/min) | 6.22 | 6.13 | 5.28 | 4.99 |
| $q_e$ (mg/g) | 24.91 | 45.11 | 62.80 | 74.27 |
| SSE | 0.589 | 1.60 | 2.95 | 5.59 |
| $\chi^2$ | 0.105 | 0.107 | 0.322 | 0.298 |
| Ritchie modified second-order model | | | | |
| $K_{2m} \times 10^{-2}$ (g/mg/min) | 6.02 | 5.92 | 5.05 | 4.76 |
| $q_e$ (mg/g) | 24.67 | 46.41 | 62.54 | 73.98 |
| $\beta$ | 1.016 | 1.023 | 1.033 | 1.041 |
| SSE | 0.461 | 1.103 | 1.523 | 3.457 |
| $\chi^2$ | 0.025 | 0.070 | 0.035 | 0.122 |

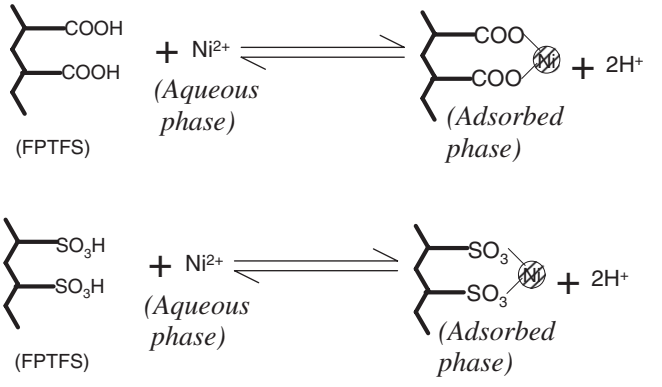


Scheme 1. Adsorption of Ni(II) onto FPTFS.

### 3.6. *Effect of ionic strength*

To explore the applicability of FPTFS for the removal of Ni(II) ions from industrial wastewaters, and also to study the nature of FPTFS/Ni(II) interaction, adsorption studies were conducted at different ionic strengths using NaCl as the electrolyte. The adsorptive removal at an initial concentration of 100 mg/L with NaCl concentration of 0.001, 0.005, 0.01, 0.05, and 0.1 M was found to be 85.1, 81.3, 76.3, 69.2 and 55.9%, respectively. The data clearly showed that FPTFS at higher ionic strength conditions exhibited a slightly decreased sorption capacity and the decreasing trend in sorption is a clear evidence for the role of electrostatic interactions in adsorption process [26]. At high ionic strength conditions, the added electrolyte provides an electrostatic shielding for Ni(II) ions at the FPTFS/solution interface through the occupation of large number of $Cl^-$ ions in the vicinity of FPTFS, causing a reduction in sorption. Earlier workers [27] reported that $Na^+$ ions compete with the metal ions for the binding sites of the adsorbent, which cause a decreased sorption at higher ionic strength. The formation of certain chloro-complexes of nickel at higher chloride concentrations is also responsible for the decreased metal uptake. Thus in general, both ion exchange and electrostatic interaction mechanisms were considered to be the major factors affecting Ni(II) adsorption on FPTFS.

### 3.7. *Adsorption isotherm analysis*

The adsorption of Ni(II) ions onto the FPTFS surface leads to a thermodynamically defined distribution of Ni(II) ions on sorbent surfaces, and this distribution can be expressed in terms of the adsorption isotherm. The experimental results for the adsorption isotherm of Ni(II) at different temperatures are shown in Figure 7. Several isotherm models were used to describe the experimental sorption data and the model parameters, along with the basic thermodynamic assumptions underlying these models, provide some insight into the sorption mechanism, surface properties and the affinity of the sorbent. Langmuir, Freundlich, Toth and Sips isotherm models were used in the present work, as shown by the following equations:

$$\text{Langmuir} : q_e = \frac{q_{m_L} K_L C_e}{1 + K_L C_e}, \tag{10}$$

$$\text{Freundlich} : q_e = K_F C_e^{1/n_F}, \tag{11}$$

$$\text{Toth} : q_e = \frac{q_{m_T} C_e}{(1/K_T + C_e^{m_T})^{1/m_T}}, \tag{12}$$

Downloaded At: 12:03 15 January 2011

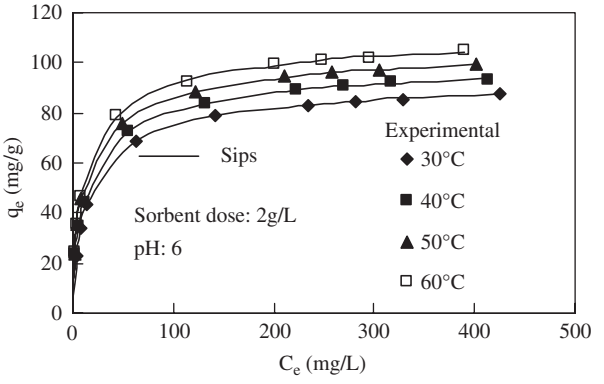


Figure 7. Comparison of the model fit of the Sips isotherm to the experimental isotherm data for the adsorption of Ni(II) onto FPTFS.

$$\text{Sips} : q_e = \frac{q_{m_S}(K_S C_e)^{m_S}}{1 + (K_S C_e)^{m_S}}, \tag{13}$$

where $q_e$ is the adsorbed amount at equilibrium (mg/g), $C_e$ the equilibrium concentration of the adsorbate (mg/L), $q_{m_L}$ is the Langmuir monolayer sorption capacity (mg/g) and $K_L$ is the Langmuir equilibrium constant (L/mg); $K_F$ is the Freundlich constant related to adsorption capacity ($mg^{1-(1/n)}L^{1/n}g^{-1}$) and $n_F$ is a constant indicative of intensity of adsorption; $q_{m_T}$ is the Toth maximum adsorption capacity (mg/g), $K_T$ the Toth equilibrium constant, and $m_T$ the Toth model exponent; $q_{m_S}$ is the Sips maximum adsorption capacity (mg/g), $K_S$ is the Sips equilibrium constant $(L/mg)^{m_S}$ and $m_S$ is the Sips model exponent.

The Langmuir model is based on the assumption that all the adsorption sites have equal affinities for adsorbate molecules and that the presence of adsorbed molecules on one site does not affect the adsorption of molecules at an adjacent site [28]. The Freundlich isotherm is an empirical equation and is satisfactory for low concentrations. The Freundlich isotherm is derived by assuming a heterogeneous surface with a non-uniform distribution of heat of adsorption over the surface [29]. The Toth isotherm is derived from the potential theory, and is applicable for a heterogeneous adsorption system [30]. The application of this equation is best suited to multilayer adsorption, similar to BET isotherms. This model also assumes that most adsorption sites have adsorption energies lower than the mean adsorption energy value. When the adsorbate molecule occupies two sorption sites, the Sips isotherm model (Langmuir–Freundlich) can be applicable [31]. At low sorbate concentrations it reduces to the Freundlich isotherm, and at higher sorbate concentrations, it predicts a monolayer sorption capacity characteristic of the Langmuir isotherm. All the isotherm parameters as determined by the nonlinear regression method and the 'goodness of fit' as manifested by SSE and $\chi^2$ are shown in Table 2.

The Langmuir monolayer sorption capacity $q_{m_L}$ and the equilibrium constant $K_L$ were found to increase from 87.56 to 102.95 mg/g and 0.079 to 0.116 L/mg, respectively, as the temperature increased from 30–60 °C. The $q_{m_L}$ value can be used to evaluate the adsorption capacity of FPTFS with other adsorbents. A comparison of the $q_{m_L}$ value of FPTFS used in the present study with those obtained in the literature shows that FPTFS is more effective for the removal of Ni(II) ions from aqueous solutions (Table 3). The relatively higher monolayer adsorption capacity of FPTFS compared to the reported adsorbents may be due to the presence of active acidic functional groups on FPTFS. The favourable nature of adsorption can be expressed in terms of a dimensionless equilibrium parameter called separation factor $R_L$, which is defined as $R_L = 1/(1 + K_L C_o)$, where $K_L$ is the Langmuir equilibrium constant and $C_o$ is the initial concentration of the Ni(II) ions in the solution. For favourable adsorption, $0 < R_L < 1$, as reported by

Downloaded At: 12:03 15 January 2011

Table 2. Adsorption isotherm constants for Ni(II) adsorption onto FPTFS.

| | Temperature (°C) | | | |
|---|---|---|---|---|
| Isotherm models | 30 | 40 | 50 | 60 |
| Langmuir | | | | |
| $q_{m_L}$ (mg/g) | 87.56 | 93.13 | 97.93 | 102.95 |
| $K_L$(L/mg) | 0.079 | 0.091 | 0.109 | 0.116 |
| SSE | 55.23 | 71.68 | 109.37 | 129.64 |
| $\chi^2$ | 1.56 | 1.88 | 2.73 | 3.27 |
| Freundlich | | | | |
| $K_F$ ($mg^{1-(1/n)}L^{1/n}g^{-1}$) | 23.25 | 25.47 | 27.76 | 29.25 |
| $n_F$ | 4.35 | 4.40 | 4.57 | 4.71 |
| SSE | 220.41 | 269.94 | 298.56 | 349.09 |
| $\chi^2$ | 4.35 | 5.09 | 5.39 | 6.11 |
| Sips | | | | |
| $q_{m_S}$ (mg/g) | 96.94 | 103.34 | 110.51 | 116.24 |
| $K_S$ $(L/mg)^{m_S}$ | 0.055 | 0.062 | 0.067 | 0.071 |
| $m_S$ | 0.714 | 0.694 | 0.658 | 0.647 |
| SSE | 0.577 | 0.192 | 0.165 | 0.211 |
| $\chi^2$ | 0.008 | 0.002 | 0.002 | 0.002 |
| Toth | | | | |
| $q_{m_T}$ (mg/g) | 100.17 | 106.94 | 115.19 | 121.33 |
| $K_T$ | 0.339 | 0.389 | 0.501 | 0.522 |
| $m_T$ | 0.591 | 0.578 | 0.533 | 0.530 |
| SSE | 1.402 | 0.902 | 0.917 | 1.333 |
| $\chi^2$ | 0.033 | 0.023 | 0.218 | 0.036 |

Table 3. Comparison of the adsorption capacities of FPTFS with various adsorbents.

| Adsorbate | Adsorbent | Modifying agent | $q_{m_L}$ | Reference |
|---|---|---|---|---|
| Ni(II) | Sawdust | Sodium hydroxide | 10.47 | [32] |
| | Jute fibres | Hydrogen peroxide | 5.57 | [33] |
| | Ground nut shell | Reactive orange 13 | 7.49 | [34] |
| | Rice bran | Phosphoric acid | 102 | [35] |
| | Bagasse fly ash | Water washed | 1.12 | [36] |
| | FPTFS | Formaldehyde | 86.74 | Present study |

Hall et al. [37]. The $R_L$ value for Ni(II) adsorption at 30, 40, 50 and 60 °C within the concentration of 50–600 mg/L varied between 0.201 and 0.020, 0.178 and 0.017, 0.154 and 0.015 and 0.146 and 0.014, respectively, indicating favourable Ni(II) adsorption on FPTFS. Freundlich adsorption constants $K_F$ and $n_F$ increased from 23.25 to 29.25 and 4.35 to 4.71, respectively, with an increase of temperature from 30–60 °C. The magnitude of $n_F$ indicates the adsorption favourability, and previous studies [38] have shown that values of $n_F$ in the range 2–10 indicate good adsorption characteristics of the adsorbent. The reported $n_F$ value for Ni(II) adsorption ($4.35 < n_F < 4.48$) confirms favourable adsorption on FPTFS. When the temperature increased from 30–60 °C, the values $q_{m_T}$ and $K_T$ increased from 100.17 to 121.33 mg/g and 0.339 to 0.522, respectively. The Toth model exponent, $m_T$, decreased from 0.591 to 0.530 with an increase in temperature from 30–60 °C. The values of $q_{m_S}$ and $K_S$ increased from 96.94 to 116.24 mg/g and 0.055 to 0.071 $(L/mg)^{m_S}$, respectively, with an increase in temperature from 30–60 °C. The Sips model exponent $m_S$ indicates surface heterogeneity and for a highly heterogeneous system, the deviation of the $m_S$ value from unity will be higher. The $m_S$ value decreased from 0.714 to 0.647 as the temperature increased from 30–60 °C, indicating that the increase in temperature made the FPTFS surface more heterogeneous, and this ultimately led to enhanced Ni(II) sorption on FPTFS.

Downloaded At: 12:03 15 January 2011

The minimum SSE and $\chi^2$ values for the Sips isotherm model compared to the other three models (Table 2) showed that the Ni(II) sorption on FPTFS could be best described by the Sips isotherm model. The experimental adsorption isotherms at temperatures 30, 40, 50 and 60 °C along with best fit Sips model curves are depicted in Figure 7. A number of investigators, Ko et al. [39] for example, have used the Sips isotherm model for the adsorption of metal ions onto bone char. Since the divalent Ni(II) ion usually prefers a 1 : 2 binding stoitiometry, as reported by earlier workers [40], the suitability of the Sips isotherm model was more obvious, because the most popular Langmuir model usually assumes a 1 : 1 binding stoitiometry for the adsorbate molecules, and when the adsorbates were divalent metal ions, this assumption suffers experimental limitations. The surface heterogeneity of FPTFS (shown by SEM photography) was another contributing factor for the misapplication of the Langmuir model for the present system because this model is best suited for homogeneous surface adsorption sites only. The aptness of the Sips isotherm model further reflects the likelihood that more than one sorption reaction/process was involved in the adsorption mechanism [41].

### 3.8. *Thermodynamic parameters*

Downloaded At: 12:03 15 January 2011

The thermodynamic parameters such as Gibb's free energy ($\Delta G_{ads}$), enthalpy ($\Delta H_{ads}$) and entropy changes ($\Delta S_{ads}$) for Ni(II) adsorption on FPTFS can be determined on the basis of the Sips equilibrium constant $K_S$ $(L/mmol)^{m_S}$ at different temperatures using the following relations:

$$\Delta G_{ads} = -RT \ln K_S, \tag{14}$$

$$\ln K_S = \frac{\Delta S_{ads}}{R} - \frac{\Delta H_{ads}}{RT}, \tag{15}$$

where R is the gas constant and T is the temperature (K). A plot of $\ln K_S$ versus 1/T should be a straight line. $\Delta H_{ads}$ and $\Delta S_{ads}$ values were obtained from the slope and intercept of this plot, respectively. The negative values (−28.52, −30.74, −33.81 and −35.67 kJ/mol) of $\Delta G_{ads}$ indicate the feasibility of the adsorption process and the spontaneous nature of adsorption of Ni(II) at 30, 40, 50 and 60 °C. The increase in negative values of $\Delta G_{ads}$ with temperature clearly showed that the Ni(II) adsorption on FPTFS was favourable at higher temperatures. Similar results were reported for the adsorption of Ni(II) ions onto various sorbents, including hazelnut shell activated carbon [42] and wine processing waste sludge [1]. The values of $\Delta G_{ads}$ for physical adsorption were $< -20$ kJ/mol and for chemisorption the values were in the range −80 to −400 kJ/mol [43]. The magnitude of adsorption free energy ranging from −28.52 to 35.67 kJ/mol suggests that the adsorption can be considered as a physical process, which was enhanced by chemical effect. The positive value of the enthalpy change $\Delta H_{ads}$ (45.93 kJ/mol) implies that the interaction between Ni(II) and FPTFS is endothermic in nature. Positive value of $\Delta S_{ads}$ (245.67 J/K/mol) corresponds to the increase in the degree of freedom at the FPTFS/Ni(II) solution interface during the adsorption process, and this also indicates that as a result of interaction between Ni(II) ions and active sites on FPTFS, some structural changes may have taken place for the latter. The isosteric heat of adsorption can be calculated using the Clausius–Clapeyron equation:

$$\frac{d(\ln C_e)}{dT} = -\frac{\Delta H_x}{RT^2}. \tag{16}$$

Here $\Delta H_x$ is the isosteric heat of adsorption (kJ/mol) at specific Ni(II) loading $q_e$ (mg/g); $C_e$ (mg/L) is the equilibrium Ni(II) concentration in the aqueous phase at temperature T. The aqueous phase Ni(II) concentrations ($C_e$) at different temperatures were calculated for a constant amount adsorbed in the FPTFS ($q_e$) using the best-fit Sips isotherm parameters listed in Table 2. The $\Delta H_x$ values were calculated from the slopes of the plots of $\ln C_e$ versus 1/T for different surface

loadings. At surface loadings of 30, 40, 50, 60, 70 and 80 mg/g, the values of $\Delta H_x$ were found to be 20.64, 20.85, 21.76, 23.67, 27.32 and 34.85 kJ/mol, respectively. The increase in the values of $\Delta H_x$ with increasing Ni(II) loading would be attributed to surface heterogeneity of FPTFS and some lateral interactions between the adsorbed Ni(II) ions [43].

### 3.9. *Tests with nickel-plating industry wastewater*

To explore the applicability of FPTFS for Ni(II) removal, batch studies were conducted at different doses of FPTFS using nickel-plating industry wastewater samples [44]. The composition of wastewater before and after treatment with an adsorbent dose of 6 g/L is given in Table 4. For comparison, batch studies were also carried out at different doses of FPTFS using 100 mg/L Ni(II) test solution. The nickel-plating industry wastewater contains a very high concentration of Ni(II) ions and hence it was diluted to a solution containing 100 mg/L during the batch process. The effect of the adsorbent dose for Ni(II) removal from the nickel-plating industry wastewater and Ni(II) test solution is shown in Figure 8. For Ni(II) test solution containing 100 mg/L Ni(II) ions, at a dose of 2 g/L, 86.6% of Ni(II) adsorption occurred, while from the nickel-plating industry wastewater, 73.2% removal was achieved. A reduction in the percentage of adsorption for the nickel-plating industry wastewater clearly implied that other ions present in the industrial wastewater were also competing for the adsorption sites on FPTFS. Almost complete removal (≈100%) for the test solution was possible at an adsorbent dose of 4 g/L, and for nickel-plating industry wastewater

Downloaded At: 12:03 15 January 2011

Table 4. Results of nickel-plating industry wastewater treatment (adsorbent dose, 6 g/L).

| Water quality parameter | Before treatment | After treatment |
|---|---|---|
| pH | 3.3 | 2.7 |
| Conductivity (ms/cm) | 13.14 | 7.02 |
| Turbidity (NTU) | 4.3 | 3.1 |
| Chemical oxygen demand (mg/L) | 51.7 | 27.6 |
| Iron (mg/L) | 35 | 28.4 |
| Sodium (mg/L) | 325 | 265.7 |
| Potassium (mg/L) | 5 | Nil |
| Calcium (mg/L) | 45 | 15.3 |
| Chloride (mg/L) | 565 | 500.6 |
| Nickel (mg/L) | 996 | <0.050 |

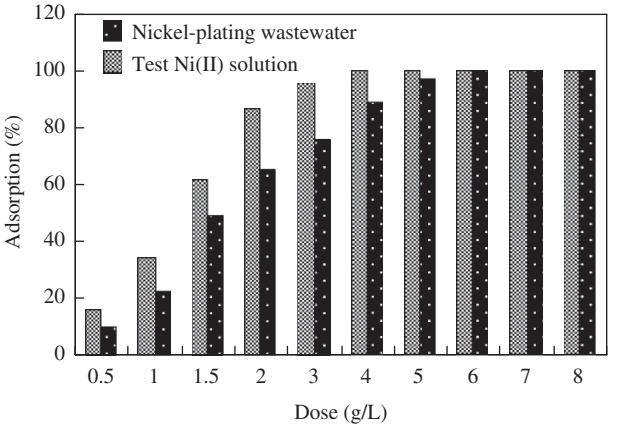


Figure 8. Comparison of the effect of adsorbent dose on the removal of Ni(II) from nickel-plating industry wastewater and test solution.

complete removal was possible at an adsorbent dose of 6 g/L. The data clearly shows that Ni(II) concentration in nickel-plating industry wastewater can be reduced to less than the permissible limit (50 μg/L) using FPTFS.

### 3.10. *Desorption and regeneration studies*

Desorption studies were conducted to check the extent of recovery of the adsorbent so that it could be used in subsequent adsorption/desorption cycles. The desorption studies also provide evidence on the reversibility of the adsorption process. The desorption of Ni(II) from FPTFS was studied by utilising 0.1 M HCl. Hydrochloric acid was selected because this eluent was reported to have the best desorption efficiency compared to many other chemical reagents [45]. Repeated adsorption/desorption cycles were performed to examine the reusability and metal recovery efficiency of the sorbent, and the results are shown in Figure 9. As shown in Figure 9 the Ni(II) adsorption capacity of the FPTFS decreased from 99.3 to 90.8% within four cycles. The recovery also decreased from 98.5–89.3% within four cycles. The results indicated that in addition to the ion exchange mechanism, certain complexation mechanisms were also involved in the adsorption process. Within four adsorption/desorption cycles no loss of the adsorbent was noticed, thus making FPTFS very suitable for the design of a continuous batch reactor.

Downloaded At: 12:03 15 January 2011

### 3.11. *Cost estimation*

Although expenditure on low-cost adsorbents may be negligible, further cost-benefit analysis needs to take into account any spending associated with regeneration or operation, including chemicals, electricity, labour, transportation and maintenance. The fiscal feasibility of the adsorption process for the removal of metal ions from water and wastewater depends on its cost effectiveness as well as the availability of adsorbents. The TFS used in the present study was collected from a local market and cost nothing. After considering the expenses for transportation, chemicals, electrical energy and labour, the final developed adsorbent would cost approximately $13.0/kg. The cost of commercially available cation exchanger Dowex (Aldrich, WI, USA) is $38.0/kg. The overall cost of treatment with FPTFS is cheaper than commercial resins. FPTFS may also be used for the removal of other metals from aqueous solutions, as the $H^+$ ions in the FPTFS can exchange with toxic metal ions and are thus expected to bring down the cost factor. Further work is ongoing to determine the effectiveness of FPTFS at removing Pb(II), Cd(II) and Zn(II) ions from aqueous solutions. This confirms the viable application of FPTFS as a low cost adsorbent.

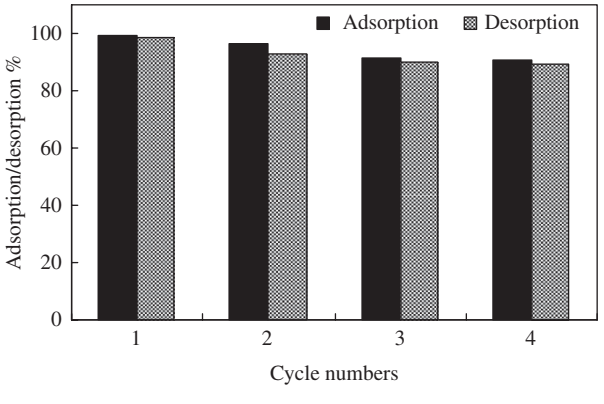


Figure 9. Four cycles of Ni(II) adsorption/desorption with 0.1 M HCl as the desorbing agent.

## 4. Conclusions

Chemically modified tamarind fruit shell can be used as a potential adsorbent to remove Ni(II) ions from aqueous solutions. The sorption of Ni(II) showed a maximum value at pH range 5–7. The adsorption kinetic data followed the Ritchie modified second-order model. The decrease of sorption capacity with increase of ionic strength showed that electrostatic interactions are mainly responsible for the adsorption process. The equilibrium data followed the Sips isotherm model and the sorption capacity increased with increase in temperature. A 1 : 2 binding stoitiometry between Ni(II) and FPTFS was followed during adsorption. The positive value of $\Delta H_{ads}$ indicated the endothermic nature of the adsorption. The magnitude of $\Delta G_{ads}$ ranged from $-28.52$ to $-35.67$ kJ/mol, which suggested that Ni(II) adsorption onto FPTFS occurred through physical interaction, and was enhanced by chemical effect. The increase in the values of the isosteric heat of adsorption with increasing Ni(II) loading on FPTFS surface evidenced the surface heterogeneity of FPTFS and some lateral interactions between the adsorbed Ni(II) ions. The complete removal of Ni(II) ions from 100 mg/L nickel-plating industry wastewater was possible with 6 g/L of FPTFS dose. Four adsorption/desorption cycles were carried out with 0.1 M HCl as the desorbing agent without loss of adsorbent or appreciable reduction in adsorption capacity.

Downloaded At: 12:03 15 January 2011

## Acknowledgements

The authors are grateful to the Professor and Head, Department of Chemistry, University of Kerala, Trivandrum for providing the laboratory facilities for this work.

## References

[1] C.C. Liu, M.K. Wang, and Y.S. Li, *Removal of nickel from aqueous solutions using wine processing waste sludge*, Ind. Eng. Chem. Res. 44 (2005), pp. 1438–1445.
[2] J.W. Patterson, *Industrial Wastewater Treatment Technology*, Butterworth, Boston, 1985.
[3] S.P. Parker, *Encyclopedia of Environmental Sciences*, McGraw Hill, New York, 1980.
[4] US EPA. *National Primary Drinking Water Regulations, Ground Water and Drinking Water*. Consumer Fact Sheet on Nickel, 1995.
[5] M.Y. Can, Y. Kaya, and O.F. Algur, *Response surface optimization of the removal of nickel from aqueous solution by cone biomass of* Pinus sylvestris, Bioresour. Technol. 97 (2006), pp. 1761–1765.
[6] E.S. Bailey, T.J. Olin, R.M. Bricka, and D.D. Adrian, *A review of potentially low-cost sorbents for heavy metals*, Water Res. 33 (1999), pp. 2469–2479.
[7] J.R. Deans and B.G. Dixon, *Uptake of $Pb^{2+}$ and $Cu^{2+}$ by novel biopolymers*, Water Res. 26 (1992), pp. 469–472.
[8] S.B. Deng, R.B. Bai, and J.P. Chen, *Aminated polyacrylonitrile fibers for lead and copper removal*, Langmuir 19 (2003), pp. 5058–5064.
[9] S.R. Shukla, R.S. Pai, and A.D. Shendarkar, *Adsorption of Ni(II), Zn(II) and Fe(II) on modified coir fibers*, Sep. Purif. Technol. 47 (2006), pp. 141–147.
[10] A. Kara, B. Acemioglu, M.H. Alma, and M. Cebe, *Adsorption of Cr(III), Ni(II), Zn(II), Co(III) ions onto phenolated wood resin*, J. Appl. Polym. Sci. 101 (2006), pp. 2838–2846.
[11] A. Ewecharoena, P. Thiravetyana, and W. Nakbanpoteb, *Comparison of nickel adsorption from electroplating rinse water by coir pith and modified coir pith*, Chem. Eng. J. 137 (2007), pp. 181–188.
[12] M.E. Argun, S. Dursuna, C. Ozdemira, and M. Karatasa, *Heavy metal adsorption by modified oak sawdust: Thermodynamics and kinetics*, J. Hazard. Mater. 141 (2007), pp. 77–85.
[13] H.L. Vasconcelosa, V.T. Fávere, N.S. Gonçalvesa, and M.C. Laranjeiraa, *Chitosan modified with Reactive Blue 2 dye on adsorption equilibrium of Cu(II) and Ni(II) ions*, React. Funct. Polym. 67 (2007), pp. 1052–1060.
[14] J.A. Schwarz, C.T. Driscoll, and A.K. Bhanot, *The zero point charge of silica-alumina oxide suspension*, J. Colloid Interface Sci. 97 (1984), pp. 55–61.
[15] K.P. Shubha, C. Raji, and T.S. Anirudhan, *Immobilization of heavy metals from aqueous solutions using polyacrylamide grafted hydrous tin(IV) oxide gel having carboxylate functional groups*, Water Res. 35 (2001), pp. 300–310.
[16] R.S. James and G.A. Parks, in *Surface and Colloidal Science*, P.J. Matpec, ed., Plenum Press, New York, 1982.
[17] M.A. Daifullah, B.S. Girgis, and H.M. Gad, *Utilization of agro-residues (rice husk) in small wastewater treatment plants*, Materials Lett. 57 (2003), pp. 1723–1731.
[18] C. Sun, R. Qu, C. Ji, Q. Wang, C. Wang, Y. Sun, and G. Cheng, *A chelating resin containing S, N and O atoms: Synthesis and adsorption properties for Hg(II)*, Eur. Polym. J. 42 (2006), pp. 188–194.

[19] A. Özer, D. Özer, and A. Özer, *The adsorption of copper(II) ions onto dehydrated wheat bran (DWB): Determination of the equilibrium and thermodynamic parameters*, Process Biochem. 39 (2004), pp. 2183–2191.
[20] F.A. Abu Al-Rub, M.H. El-Nass, F. Benyahia, and I. Ashour, *Biosorption of nickel on blank alginate beads, free and immobilized cells*, Process Biochem. 39 (2004), pp. 1767–1773.
[21] B.F. Noeline, D.M. Manohar, and T.S. Anirudhan, *Kinetic and equilibrium modeling of lead(II) sorption from water and wastewater by polymerized banana stem in a batch reactor*, Sep. Purif. Technol. 45 (2005), pp. 131–140.
[22] S. Lagergren, *About the theory of so-called adsorption of soluble substances*, K. Vetenskapsakad. Handl. 24 (1898), pp. 1–39.
[23] A.G. Ritchie, *Alternative to the Elovich equation for the kinetics of adsorption of gases on solids*, J. Chem. Soc. Farad .Trans. 73 (1977), pp. 1650–1653.
[24] C.W. Cheung, J.F. Porter, and G. McKay, *Elovich equation and modified second-order equation for sorption of cadmium ions onto bone char*, J. Chem. Technol. Biotechnol. 75 (2000), pp. 963–970.
[25] B.S. Inbaraj and N. Sulochana, *Carbonised jackfruit peel as an adsorbent for the removal of Cd(II) from aqueous solution*, Bioresour. Technol. 94 (2004), pp. 49–52.
[26] A.J. O'Connor, A. Hokura, J.M. Kisler, S. Shimazu, G.W. Stevens, and Y. Komatsu, *Amino acid adsorption onto mesoporous silica molecular sieves*, Sep. Purif. Technol. 48 (2006), pp. 197–201.
[27] N. Fiol, I. Villaescusa, M. Martínez, N. Miralles, J. Poch, and J. Serarols, *Sorption of Pb(II), Ni(II), Cu(II) and Cd(II) from aqueous solution by olive stone waste*, Sep. Puri. Technol. 50 (2006), pp. 132–140.
[28] I. Langmuir, *The adsorption of gases on plane surfaces of glass, mica and platinum*, J. Am. Chem. Soc. 40 (1918), pp. 1361–1403.
[29] H.M.F. Freundlich, *Over the adsorption in solution*, J. Phys. Chem. 57 (1906), pp. 385–470.
[30] J. Toth, *State equations of the solid gas interface layer*, Acta. Chem. Acad. Hung. 69 (1971), pp. 311–317.
[31] R. Sips, *On the structure of a catalyst surface*, J. Chem. Phys. 16 (1948), pp. 490–495.
[32] Habib-ur- Rehman, M. Shakirullah, I. Ahmad, S. Shah, and Hamedullah, *Sorption studies of nickel ions onto sawdust of* Dalbergia sissoo, J. Chin. Chem. Soc. 53 (2006), pp. 1045–1052.
[33] S.R. Shukla and R.S. Pai, *Adsorption of Cu(II), Ni(II) and Zn(II) on modified jute fibres*, Bioresour. Technol. 96 (2005), pp. 1430–1438.
[34] S.R. Shukla and R.S. Pai, *Adsorption of Cu(II), Ni(II) and Zn(II) on dye loaded groundnut shells and sawdust*, Sep. Purif. Technol. 43 (2005), pp. 1–8.
[35] M.N. Zafar, R. Nadeem, and M.A. Hanif, *Biosorption of nickel from protonated rice bran*, J. Hazard. Mater. 143 (2007), pp. 478–485.
[36] V.K. Gupta, C.K. Jain, I. Ali, M. Sharma, and V.K. Saini, *Removal of cadmium and nickel from wastewater using bagasse fly ash – a sugar industry waste*, Water Res. 37 (2003), pp. 4038–4044.
[37] K.R. Hall, L.C. Eagleton, A. Acrivos, and T. Vermeulen, *Pore and solid diffusion kinetics in fixed-bed adsorption under constant pattern conditions*, Ind. Eng. Chem. Fundam. 5 (1966), pp. 212–223.
[38] R.E. Treybal, *Mass-transfer Operations*, 3rd ed., McGraw-Hill, New York, 1981.
[39] D.C. Ko, C.K. Porter, and G. Mckay, *Optimised correlations for the fixed-bed adsorption of metal ions on bone char*, Chem. Eng. Sci. 55 (2000), pp. 5819–5829.
[40] S. Schiewer and M.H. Wong, *Metal binding stoichiometry and isotherm choice in biosorption*, Environ. Sci .Technol. 33 (1999), pp. 3821–3828.
[41] D.C. Ko, C.K. Porter, and G. Mckay, *Mass transport model for the fixed bed sorption of metal ions on bone char*, Ind. Eng. Chem. Res. 42 (2003), pp. 3458–3469.
[42] E. Demirbas, M. Kobya, S. Oncel, and S. Sencan, *Removal of Ni(II) from aqueous solution by adsorption onto hazelnut shell activated carbon: Equilibrium studies*, Bioresour. Technol. 84 (2002), pp. 291–293.
[43] M.R. Unnithan, and T.S. Anirudhan, *The kinetics and thermodynamics of sorption of chromium(VI) onto the iron(III) complex of a carboxylated polyacrylamide-grafted sawdust*, Ind. Eng. Chem. Res. 40 (2001), pp. 2693–2701.
[44] K. Kadirvelu, K. Thamaraiselvi, and C. Namasivayam, *Removal of heavy metals from industrial wastewaters by adsorption onto activated carbon prepared from an agricultural solid waste*, Bioresour. Technol. 76 (2001), pp. 63–65.
[45] T. Godjevargova, A. Simeonova, and A. Dimov, *Adsorption of heavy metal ions from aqueous solutions by porous polyacrylonitrile beads*, J. Appl. Polym. Sci. 83 (2002), pp. 3036–3044.

Downloaded At: 12:03 15 January 2011